Effect of TID-dressing on Fatigue Life Stress Concentration Factor in St37-2Butt Weldments

Abbas Fadaei*
Department of Mechanical Engineering,
University of Bu-Ali Sina, Iran
E-mail: fadaei@basu.ac.ir
*Corresponding author

Mostafa Jalali Zadeh, Faezeh Mohammad Zaheri

Department of Mechanical Engineering,
University of Bu-Ali Sina, Iran
E-mail: mostafajalalizadeh@yahoo.com, mz_faeze@yahoo.com

Received: 21 February 2018, Revised: 30 April 2018, Accepted: 10 July 2018

Abstract: The researchers have shown that there are cracks in the toe weld and they have an important role in the welding failure. The elimination of these shortcomings and the improvement of the fatigue life have always been a concern for the industrial designers. One method of improving the fatigue life of the welded joint at its geometry branch is to remelt the toe region of the steel weldments using the Tungsten Inert Gas (TIG) method or TIG-dressing. This method affects the material structure, hardness, stress coefficient and welding shape. In this study, the effectiveness of this method on fatigue and stress concentration at the weld toe was investigated. The experimental results showed that the toe weld form was changed by TIG – dressing and thus increased the radius and decreased the toe weld's angle, so that the stress was reduced by TIG – dressing. Also, the fatigue tests showed that the fatigue life increased by an average of approximately 30 percent. Finally, the stress concentration factors were obtained using ABAQUS finite element analysis. The amount of stress concentration factors in weldments before and after TIG – dressing were respectively achieved to be 2.4 and 1.3.

Keywords: Butt Welded Joint, Fatigue Life, Stress Concentration Factor, TIG-Dressing

Reference: Fadaei, A., Jalali Zadeh, M., and Mohammad Zaheri, F., "Effect of TID-dressing on Fatigue Life Stress Concentration Factor in St37-2Butt Weldments", Int J of Advanced Design and Manufacturing Technology, Vol. 12/No. 1, 2019, pp. 113–121.

Biographical notes: A. Fadaei received his PhD in Mechanical Engineering from Bu-Ali Sina University. He is currently Assistant Professor at the Department of Mechanical Engineering, Bu-Ali Sina University, Hamedan, Iran. His current research interest includes Stress Analysis and Applied Design. **M. Jalali Zadeh** received his MSc in Mechanical Engineering from Bu-Ali Sina University, IRAN, in 2015. His research field is Applied Design and Stress Analysis. **F. Mohammad Zaheri** received both BSc and MSc in Mechanical engineering from Bu-Ali Sina University, IRAN, in 2012 and 2015, respectively. Her research interest is Computational Mechanic Problems.

1 INTRODUCTION

The low fatigue strength of the welded joints is caused by several factors; the most important ones being, firstly, the stress concentration caused by the geometry of the weld bead, and secondly, the defects in the toe region consisting of crack-like non-metallic intrusions. Therefore, the fatigue cracks start growing very early during service. The useful life of the structure consists mainly of the propagation of such cracks to some critical value at which the static fracture takes place. The crack growth rate is largely independent of the static strength; thus, welded high strength steels cannot be expected to exceed the fatigue performance of low strength steel, unless the weld is improved in such a way that the crack initiation stage occupies a large portion of the fatigue life. Several techniques have been developed to improve the fatigue properties of the welds. The most effective methods are those that change the geometry of the weld, thereby reducing the stress concentration factor. In the branch of geometry modification, one method to improve the fatigue life of the weldments is TIG-Dressing. Using this method, the welding toe remelts and the geometry of the weld bead changes.

Several researchers have studied TIG-Dressing method. Huo et al [1] investigated the fatigue behaviour of the welded joints treated by TIG-dressing and ultrasonic peening under variable-amplitude load. Perović [2] studied TIG-dressing treatment and showed that the amount improvement depends on the metal base, connection type and also load type. Tateishiet al [3] improved extremely low cycle fatigue strength of the welded joints by toe finishing. Ramalho et al [4] investigated the effect of TIG-dressing and plasma-dressing on the fatigue strength of welded parts. Li et al [5]-[6] examined the effect of TIG-dressing on low-strength steel Q235B to improve the fatigue property.

Lee and Chang [7] examined the growth rate of the fatigue cracks in the welded butt using the finite element method. The results demonstrated the significance of the residual stresses in the assessment of the fatigue crack growth rate in the welds. Furthermore, Fang [8] examined such methods as TIG-dressing, shot blasting, the creation of compressive residual stress by ultrasonic peening and etc. to improve the fatigue strength of the welded structures. Using TIG-dressing, Zhou et al [9] investigated the effect of cooling on the welding residual stress in the modified T-shaped pieces performed. The results showed that by increasing the intensity of cooling, the longitudinal tensile residual stress converted to the compressive stress and the transverse residual stress did not change.

Wu and Wang [10] improved the fatigue performance of the welded joints with undercuts by TIG-Dressing treatment. Gerritsen et al [11] examined diode laser weld toe remelting as a means of fatigue strength improvement in high strength steels. Es and et al [12-13] investigated the effect of TIG-dressing on fatigue strength of the welded joints in S460 and S1100 and indicated that the average welding with TIG-dressing had a positive effect on the weld toe's geometry. Also, it should be noted that the hardness increase is another result of the TIG-dressing method.

Yildrim [14] pointed out that the experimental fatigue data for the welds improved via the tungsten inert gas (TIG) dressing method, have been extracted from the existing literature. The extracted fatigue data include experimental points for the longitudinal attachments, transverse non-load carrying welds, butt joints and T-joints. Hildebrand et al [17] performed a numerical simulation of TIG-dressing method in the welded joints. The results showed that the method reduced the residual stress surface on the joints.

The overriding purpose of this study is to investigate the effect of TIG-dressing on the fatigue life and stress concentration factor in St37-2 butt weldments. Two reasons have encouraged the present researchers to study this material. First, it is highly utilized in the industry and second, it has not been studied in the previous research. The fatigue tests on the specimens were done and the results are discussed accordingly. Another purpose of this study is to investigate the impact of TIG-dressing on the stress concentration factor at the weld toe using the finite element simulation.

The difference between this study and previously done studies and also the innovations carried out in this research, is the simulation of the TIG-dressing method and the extraction of changes in the coefficient of stress concentration before and after correction as the main factor of the effect of this method on increasing the fatigue life expectancy by finite element method and using ABAQUS software. As it was stated before, the study made use of steel St37-2 which are widely used for the construction of welded parts. In this respect, this experimental study examines the effect of TIG-dressing on the fatigue life in the presence of the crack-like defect. This procedure - creating the crack-like defect with the elliptical geometry - cannot be seen in the literature. To this aim, the finite element simulation, using sub-model with code-writing in the software environment was chosen as the new approach of this study.

2 EXPERIMENTAL STUDY

To prepare the experimental specimens, the St37-2 sheets with a thickness of 8 mm were used. Initially two sheets were welded together, and then specimens were cut from welded sheets. Some specimens were treated by TIG-dressing. Finally, a specific defect was created in all of the specimens before the fatigue tests. In the

following section the specimens' preparation is described in detail.

Welding process: In order to prepare specimens, two sheets with the dimensions of 250×125 mm and the thickness of 8 mm were welded using manually submerged-arc welding (SAW) method. The edges of sheets in the welding region were chamfered using a CNC machine. The electrode type E7018 with a diameter of 5 mm was used for the four-pass welding. The conditions of welding operation were selected based on the AWS D1.1 standard. [19] According to this standard, butt-weld geometry is shown in "Fig. 1" [19]. Geometric characteristics of the welded sheets and welding conditions are displayed in "Table 1 and Table 2", respectively.

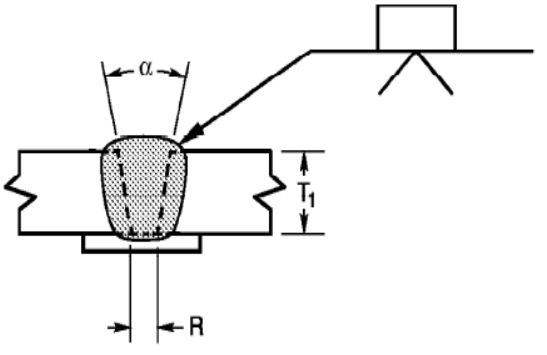

Fig. 1 Butt weld geometry according to standard AWS D1.1 [19].

Cutting and milling of specimens: After the welding operation, the fatigue specimens were cut using a Wire Cut Machining (WCM) and were milled by CNC milling machine for getting detailed dimensions. The view of the specimen is shown in "Fig. 2".

Table 1 Transitions selected for thermometry [19]

Welding Process	Base Metal Thickness (U=unlimited)	Groove Preparation		Allowed Welding Position
	T_1	Root Opening, in	Groove Angle	
SMAW	U	R= $\frac{1}{4}$	$\alpha = 45^{o}$	All

TIG-dressing operation: First, the specimens were preheated to 150 °C for 30 minutes inside the furnace. Then, according to the TIG-dressing equipment, the distance of tungsten electrode from weld bead was selected to be approximately 1 mm. After the operation, the welding toe radius was measured. It was equivalent to 3.5 mm. The conditions of TIG-dressing operation are indicated in "Table 3".

Table 2 Welding condition

Passes	Voltage, V	Current, A	Velocity, mm/s
1	21.5	95	2.25
2	21.5	112	2.30
3	21.5	112	2.83
4	21.5	112	2.50

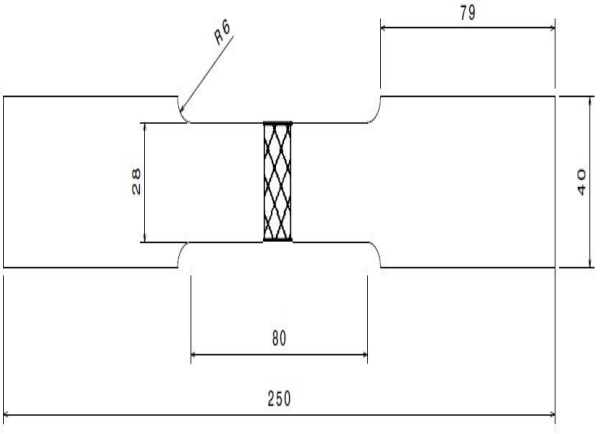

Fig. 2 The view of the fatigue specimen, mm.

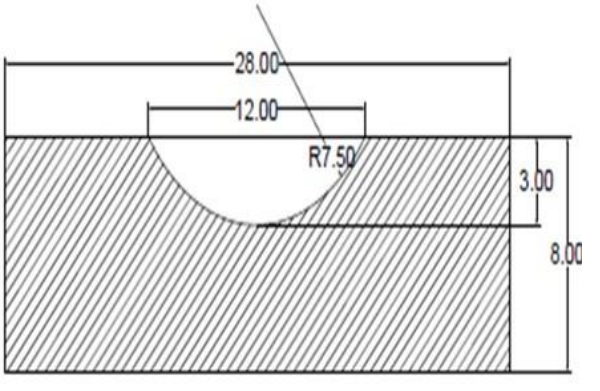

Fig. 3 The cross-section of quasi-elliptical defect in the specimen, mm.

Table 3 Conditions of TIG-dressing operation

Insert gas	Argon
Gas flow, lit/min	8
Nozzle diameter, mm	10
Preheat temperature, ºC	150
Electrode diameter, mm	4
Voltage, V	14
Current, A	200
Velocity, mm/min	150

Production defect in samples: After TIG-Dressing, for fatigue test, the quasi-elliptical defect (an arc of a circle as shown in "Fig. 3") was created at the weld toe by the Electrical Discharge Machining (EDM). The closed view of the defect in the specimen is displayed in "Fig. 4". Also, "Fig. 5 and 6" display specimens without and with TIG-dressing, respectively.

Fatigue test: The specimens were tested by INSTRON fatigue machine. In the fatigue tests, the maximum stress 382 MPa, the stress ratio 0 and the frequency of 3 Hz were selected. In order to ensure the repeatability of the test results, three specimens without and with TIG-dressing were tested. The specimen after the failure is shown in Figure 7.

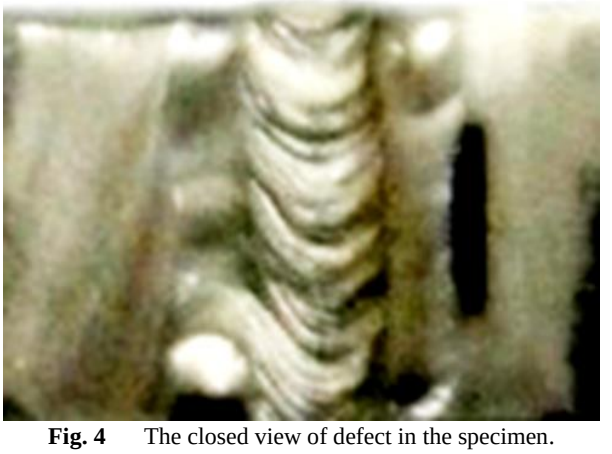

Fig. 4 The closed view of defect in the specimen.

Fig. 5 The specimen after the failure.

3 FINITE ELEMENT ANALYSIS

The welding and TIG-dressing treatments were simulated using finite element software ABAQUS in accordance with the experiments for calculating the stress concentration factors in the weldments before and after TIG-dressing operation.

Welding process simulation: First, two sheets and four passes of welding were modelled. This model is shown in "Fig. 6". The thermal properties of the sheets and welding filler as temperature-dependent were obtained in the finite element analysis [15]. The heat load caused by the welding source was defined in the form of a volumetric heat flux and in accordance with the conditions in the experimental work. Goldak's two ovals moving heat source model [18] was chosen to create the heat generated by an electrode. In order to apply the heat flux, a subroutine was produced in a way that all conditions in an experimental work such as the flow rate, the electric potential difference, the speed of the electrode and the electrode center position at any moment were applied. The heat flux contained two zones, one in front and the other in behind of the arch's center. The two elliptical-shaped flux distribution power densities are shown in "Fig. 7".

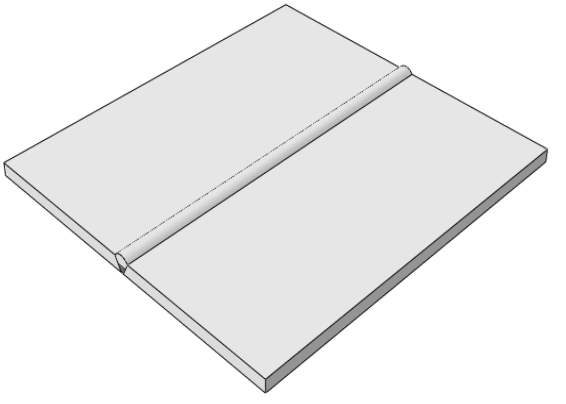

Fig. 6 Modelling of two sheets and four passes pf welding.

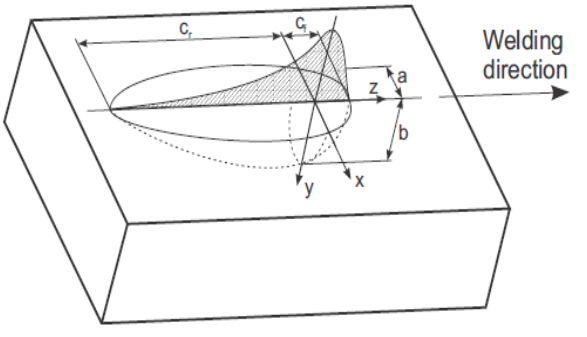

Fig. 7 The elliptical-shaped flux distribution power density [18].

The power density distribution of the front center of the arc is described by "Eq. (1)" [18]:

$$q(x,y,z,t)=\frac{6\sqrt{3}f_f Q}{abc_f\pi\sqrt{\pi}}e^{-3x^2/a^2}e^{-3y^2/b^2}e^{-3[z+v(\tau-t)]^2/c_f^2} \quad (1)$$

In a similar vein, the power density distribution of the rear center of the arch is represented by "Eq. (2)" [18]:

$$q(x,y,z,t)=\frac{6\sqrt{3}f_r Q}{abc_r\pi\sqrt{\pi}}e^{-3x^2/a^2}e^{-3y^2/b^2}e^{-3[z+v(\tau-t)]^2/c_r^2} \quad (2)$$

In these equations, the geometric parameters a, b, cf and cr as physical dimensions of melting zone at respectively the side, below, front and rear were determined from cutting and polishing-etching the cross-section of the weldment. The other described parameters including f_f and fr were obtained from [18].

"Fig. 8" shows how to apply the heat flux to the model at the end of the fourth pass of welding, i.e. at the time of 1450 seconds after the analysis.

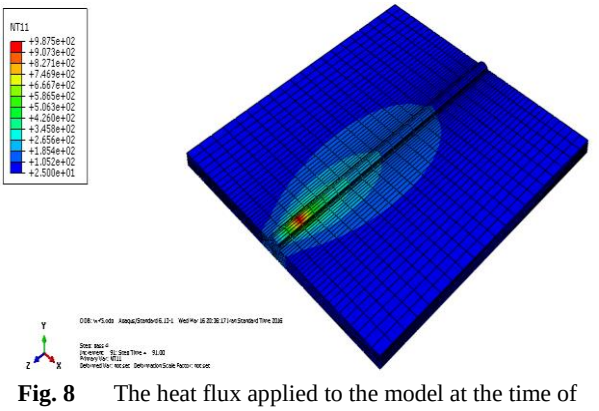

Fig. 8 The heat flux applied to the model at the time of 1450 seconds.

The temperature distribution versus time in the specific point with the distance of 10 mm from the weld line is shown in "Fig. 9". As shown in this Figure, the temperature distribution of the welding process may be divided into three stages: before reaching the heat source, passing the heat source and the cooling stage. Until the heat source had not reached the point, the temperature was almost constant, but as the heat source approached, the temperature suddenly increased. In addition, because of the effect of radiation heat transfer in high-temperature, the temperature decreased quickly after passing the heat source. For the next pass, this process was repeated until the end of the fourth pass.

In the following, the mechanical analysis was performed. The type of the element was selected as C3D8R for the mechanical analysis. Figure 10 shows the distribution of Von-Mises stress at the end of the fourth pass.

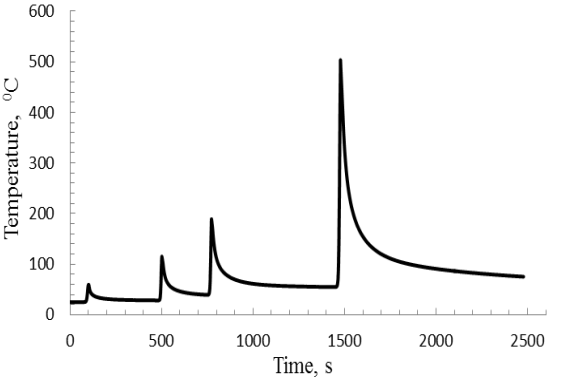

Fig. 9 Temperature distribution versus time at the specific point with the distance of 10 mm from the weld line.

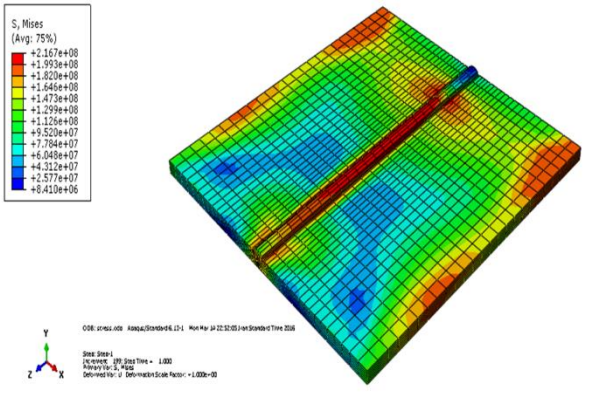

Fig. 10 The welding residual stress distribution in the model.

Validation of the simulation method: In order to gain more accurate evaluation of the results of the finite element analysis, the results obtained from this study were compared with those obtained in Nuraini and et al [16]. The transverse residual stress distribution derived from the simulation and extracted from [16], is compared in "Fig. 11". As shown in this Figure, the trend of the results of the simulation and that of [16] is almost the same. The difference arises from a lack of full access to the detailed data used in the analysis by [16].

Cutting Specimen: As mentioned before, the sheets were initially welded and then the specimens were cut from them for the fatigue tests. The sample is shown in "Fig. 12". In this part of the simulation, to perform this process, the sub-model was used. After the welding simulation, the stresses were transferred from the welding sheets to the sample for analysing the sub-

model by using a static step. Von-Mises stress distribution in the sample after analysing is shown in "Fig. 13".

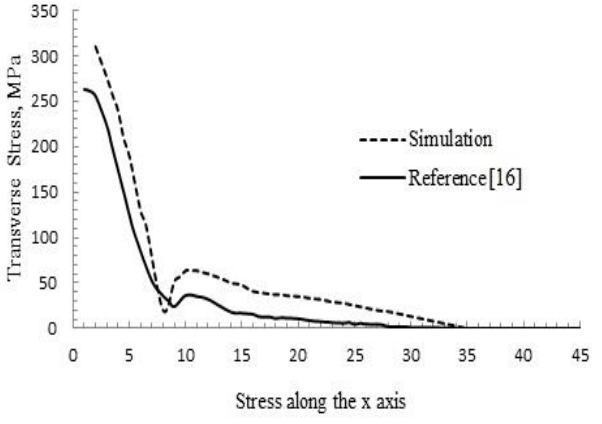

Fig. 11 Comparison between the results of the simulation and reference [16].

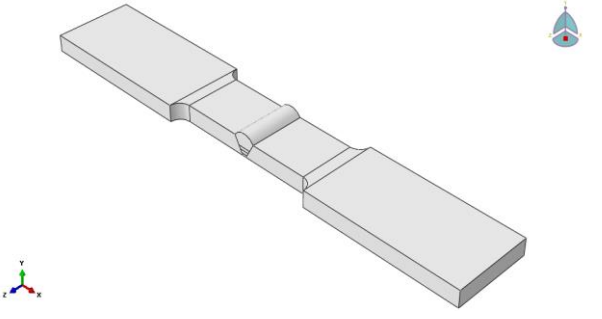

Fig. 12 The sample cut from the sheets.

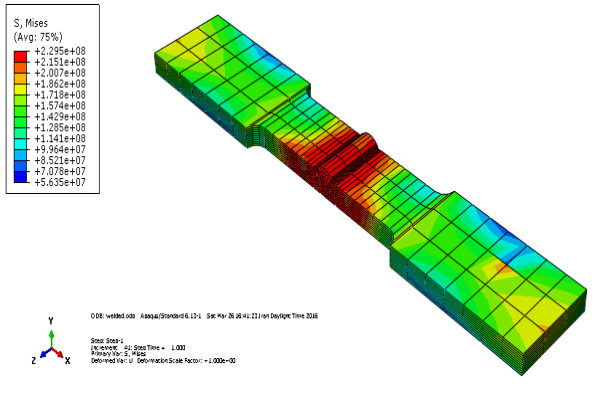

Fig. 13 Von-Mises stress distribution in the sample.

The finite element simulation of TIG-dressing: To simulate the TIG-dressing, the model obtained from the sub-model was used. To accomplish this step, the thermal-mechanical coupled method was used. The type of the element used in this solution was selected to be C3D8T which is capable of solving the heat transfer and stress analyses, simultaneously. In order to transfer the pattern of residual stresses from the sub-model to the TIG-dressing mesh, this mesh was considered entirely similar to the sub-model. For this purpose, the birth and death of the elements' technique were used to show the melted zone. The initial temperature of 150 C was considered. Figure 14 shows one step of the finite element simulation of TIG-dressing. Also, the distribution of Von-Mises residual stress distribution in the sample after TIG-dressing operation is represented in "Fig. 15". By comparing "Fig. 13 and 15", it can be seen that although the maximum stress is increased, the stress distribution becomes more uniform by TIG-dressing operation. Also, the stresses in Heat Affected Zone (HAZ) decreases after implementing TIG-dressing method.

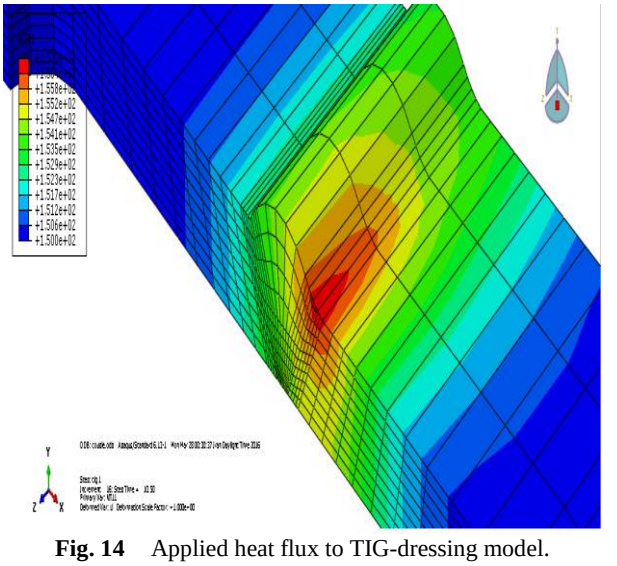

Fig. 14 Applied heat flux to TIG-dressing model.

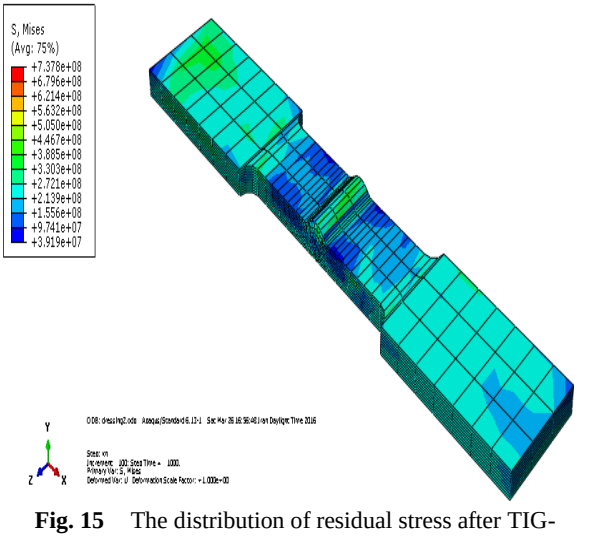

Fig. 15 The distribution of residual stress after TIG-dressing.

Analysis of stress concentration factor: At the end of the simulation, the stress concentration at the weld toe in the samples was calculated in the unmodified and modified samples using TIG-dressing. In order to determine the stress concentration in both cases, the tensile load was applied to the samples. The tensile load applied to the sample was considered to be equal to 70 MPa. After the analysis, the paths were defined in the modification zone and also in the area away from it and the stresses were extracted in the paths. This path in unmodified and modified samples is shown in "Fig. 16 (a) and 16 (b)" respectively. Finally, the stress concentration factor was calculated by dividing the maximum value of stress at the weld toe to the nominal stress in a region far from that.

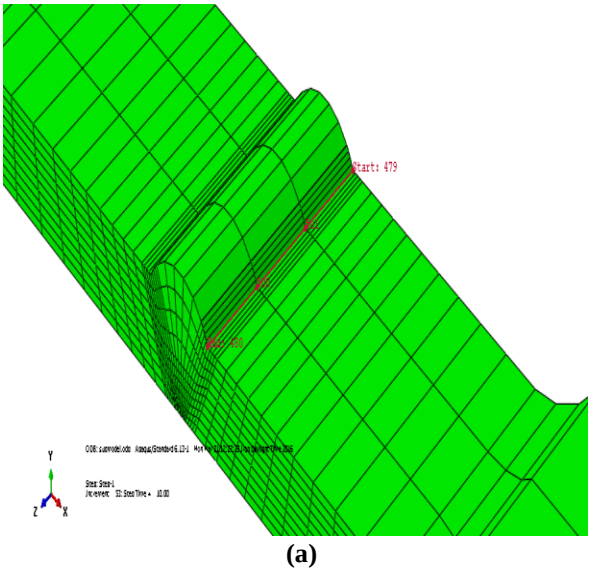

(a)

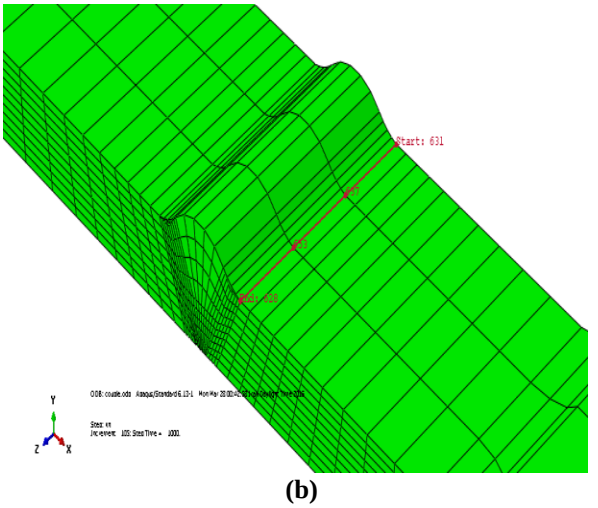

(b)

Fig. 16 The path in: (a): unmodified and (b): modified, sample.

4 RESULTS AND DISCUSSION

Experimental results: The results obtained from the Fatigue test are shown in "Table 4". The results expressed that with TIG-dressing, the average fatigue life of three tested specimens increased from 27415 cycles to 35584 cycles, i.e. approximately 30 percent. Also the radius of the toe weld was measured before and after the TIG-dressing. Before the correction, it was 1.2 mm and after that it was 3.5 mm. therefore, as these values suggest, the toe weld increased after TIG-dressing.

Table 4 The fatigue results

Specimens	Fatigue life, cycles			Average Fatigue life, cycles
	First test	Second test	Third test	
Without TIG-dressing	26973	25077	30196	27415
With TIG-dressing	34011	33270	39471	35584

The cross-section of one of the specimens without and with TIG-dressing after the failure is shown in "Fig. 17 (a) and 17 (b)", respectively. As shown in the figures, the fracture surface is divided into three areas: crack initiation region (I), crack growth area (II) and brittle fracture zone (III). The crack growth region was smoother than the brittle fracture zone. The crack growth area of the specimen with TIG-dressing was larger than that of the specimen without TIG-dressing. That is to say, the fatigue life increases by TIG-dressing.

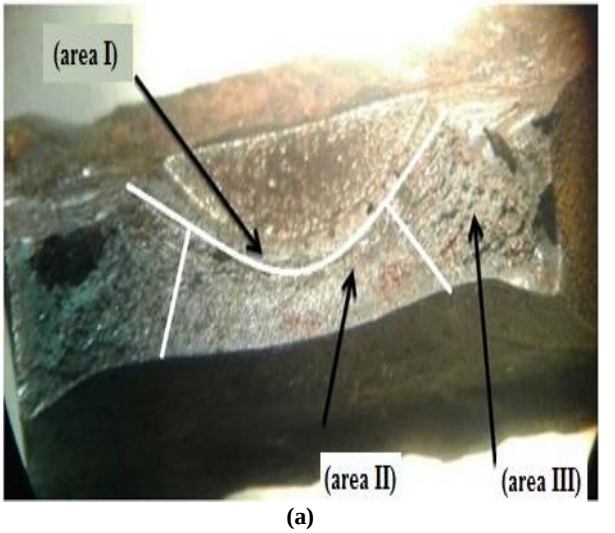

(a)

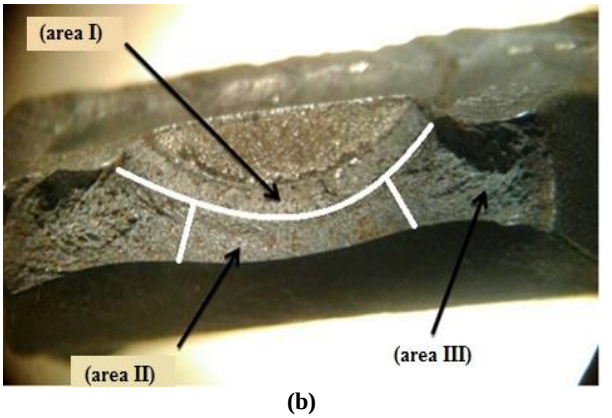

(b)

Fig. 17 The cross-section of the specimen with TIG-dressing after the failure.

Simulation results: Von-Mises residual stresses along the weld line for before and thereafter applying TIG-dressing are shown in "Fig. 18". By comparing the two graphs, it can be seen that the surface residual stresses along the weld line is reduced. Therefore, by reducing the surface residual stress in the sample, it takes more time to initiate and to grow cracks on the surface which consequently leads to gaining the fatigue strength and fatigue life in the samples. Also, the stress concentration factors for the unmodified and modified samples were computed and are shown in "Table 5". The results showed that with TIG-dressing operation, the stress concentration factor reduced and thus the fatigue life increased.

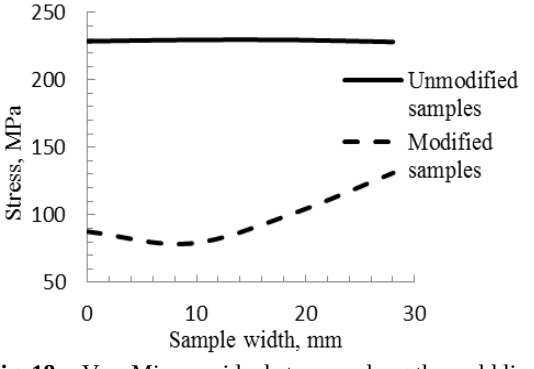

Fig. 18 Von-Mises residual stresses along the weld line.

Table 5 Stress concentration factor

Before TIG-dressing operation	After TIG-dressing operation
2.40	1.32

5 CONCLUSION

In this study, the effect of TIG-dressing operation in the weld fatigue life of St37-2 butt weldment was investigated experimentally and the stress concentration factor of the sample in accordance with the experiments was simulated numerically. The following results were obtained:

1- Through TIG-dressing operation for modifying the weldments, the residual stress decreased in surface. For this reason, it took more time to initiate and to grow cracks on the surface which consequently led to the fatigue strength to be increased and the fatigue life to be obtained. For St37-2 weldment, the specimens and defined conditions of welding and TIG-dressing operations, the average fatigue life increased from 27415 cycles for the unmodified sample to 35584 cycles for the modified sample, i.e. approximately 30 percent.

2- By implementing TIG-dressing method, the weld toe shape changed which increased the radius and decreased the toe weld's angle. Under all circumstances described in this study, for the specimen and the operations mentioned above, this deformation reduced the stress concentration factor from 2.40 to 1.32 in the sample.

3- It can be seen that although the maximum stress increased, the stress distribution became more uniform by TIG-dressing operation. Also, the stresses in Heat Affected Zone (HAZ) decreased after implementing the TIG-dressing method.

REFERENCES

[1] Huo, L., Wang, D., and Zhang, Y., Investigation of the Fatigue Behaviour of the Welded Joints Treated by TIG Dressing and Ultrasonic Peening under Variable-Amplitude Load, International Journal of Fatigue, Vol. 27, No. 1, 2005, pp. 95-101.

[2] Perović, Z. D., Investigation of the Fatigue Strength of the Welded Joints Treated by TIG Dressing, Archives of Materials Science, Vol. 28, 2007, 113-117.

[3] Tateishi, K., Hanji, T., and Hanibuchi, T., Improvement of Extremely Low Cycle Fatigue Strength of Welded Joints by toe Finishing, Welding in the World, Vol. 53, No 9-10, 2009, pp. R238-R45.

[4] Ramalho, A. L., Ferreira, J. A. M., and Branco, C., Fatigue Behaviour of T-Welded Joints Rehabilitated by Tungsten Inert Gas and Plasma Dressing, Materials & Design, Vol. 32, No. 10, 2011, pp. 4705-4713.

[5] Li, D. X., Jia, B. C., and Zhu, Y. Z., Enhancement of the Fatigue Property of the Crack of Cruciform Welded Joints by TIG-Dressing, Advanced Materials Research, Vol. 146-147, 2011, pp. 1419-1422.

[6] Li, C. R., Cao, Z. P., and Fang, Z. T., Research on Methods of Improving Fatigue Property of Low-Strength Steel Welded Joints, Applied Mechanics and Materials, Vol. 538, 2014, pp. 48-53.

[7] Lee, C. H., Chang, K. H., Finite Element Computation of Fatigue Growth Rates for Mode I Cracks Subjected to

Welding Residual Stresses, Engineering Fracture Mechanics, Vol. 78, No. 13, 2011, pp. 2505-2520.

[8] Fang, Z. T., Research Progress of Methods to Improve Fatigue Strength of Welded Structures, Applied Mechanics and Materials, Vol. 217-219, 2012, pp. 1614-1617.

[9] Zhou, K., Shi, C. Y., and Jin, C., Influence of Cooling Intensity on Residual Stress State of TIG Dressing Zone for T-Joint Welded Toe, Applied Mechanics and Materials, Vol. 148-149, 2012, pp. 1289-1294.

[10] Wu, L. C., Wang, D. P., Improve the Fatigue Performance of Welded Joints with Undercuts by TIG-Dressing Treatment, Advanced Materials Research, Vol. 472-475, 2012, pp. 1300-1304.

[11] Gerritsen, C., Vanrostenbergh, S., and Doré, M., Diode Laser Weld Toe Re-Melting as a Means of Fatigue Strength Improvement in High Strength Steels, Procedia Engineering, Vol. 66, 2013, pp. 171-180.

[12] Van Es, S. H. J., Kolstein, M. H., Pijpers, R. J. M., and Bijlaard, F. S. K., TIG-Dressing of High Strength Steel Butt Welded Connections – Part 1: Weld Toe Geometry and Local Hardness, Procedia Engineering, 5th International Conference on Fatigue Design, Vol. 66, 2013, pp. 216-225.

[13] Van Es, S. H. J., Kolstein, M. H., Pijpers, R. J. M., and Bijlaard, F. S. K., TIG-Dressing of High Strength Butt Welded Connections – Part 2: Physical Testing and Modelling, Procedia Engineering, Vol. 66, 2013, pp. 126-37.

[14] Yildrim, H. C., Review of Fatigue Data for Welds Improved by Tungsten Inert Gas Dressing, International Journal of Fatigue, Vol. 79, 2015, pp. 36-45.

[15] Barsoum, Z., Barsoum, I., Residual Stress Effects on Fatigue Life of Welded Structures Using LEFM, Engineering Failure Analysis, Vol. 16, No. 1, 2009, 449-467.

[16] Nuraini, A. A., Zainal, A. S. M., and Azmah Hanim, M., The Effect of Welding Process Parameter on Temperature and Residual Stress in Butt-Joint Weld of Robotic Gas Metal Arc Welding, Australian Journal of Basic and Applied Sciences, Vol. 7, No. 7, 2013, 814-820.

[17] Hildebrand, J., Starcevic, I., Werner, F., Heinemann, H., and Köhler, G., Numerical Simulation of TIG-Dressing of Welded Joints, International Conference on Computing and Decision Making in Civil and Building Engineering, Montréal, Canada, 2006.

[18] Goldak, J. A., Akhlaghi, M., Computational Welding Mechanics, Springer, USA, 2005.

[19] AWS, D1.1/D1.1M, Structural Welding Code-Steel. American Welding Society, 2015.